ELECTROWEAK PHYSICS AT HERA

J. MEYER

Deutsches Elektronen Synchrotron DESY
Notkestrasse 85, 22607 Hamburg, Germany
E-mail: joachim.meyer@desy.de

Results obtained at HERA concerning electroweak physics in deep inelastic electron-proton scattering are reviewed. At HERA I electroweak unification has been demonstrated. In a global fit to the measured proton structure functions QCD and electroweak parameters are determined simultaneously. The availibility of polarised electrons at HERA II allows to determine the chirality properties of NC and CC interactions at high spacelike momentum transfers.

1. Results from the HERA I phase

1.1. *NC and CC cross sections*

The electron proton collider HERA operates since 1993 at center of mass energies above 300 GeV. Already the very first data accumulated in 1993 allowed to observe the charged current (CC) deep inelastic scattering (DIS) process at high spacelike momentum transfers Q^2 and established the W propagator effect [1]. Figure 1 shows the then measured CC cross section converted to an equivalent fixed target neutrino nucleon scattering cross section. The cross section clearly deviates from a linear rise indicating the finite mass in the spacelike W propagator.

In the HERA I phase (1993 - 2000) both experiments, H1 and ZEUS, accumulated more than 100 pb^{-1} each in e^+p and e^-p scattering. This amount of luminosity allowed to study electroweak effects extending into kinematic regions where the four momentum tranfer Q exeeds the masses of the gauge bosons W and Z. Figure 2 shows the cross sections [2,3] differential in Q^2 for NC and CC processes in e^+p and e^-p scattering. Whereas the NC cross sections exeeds the CC cross section at low values of Q^2 by several orders of magnitude they become similar in the region where $Q^2 \sim M_W^2, M_Z^2$. This is the first direct demonstration of electroweak unification in spacelike DIS scattering. Figure 2 also shows the sensitivity of the cross sections to the lepton charge. In NC scattering the cross section difference arises from the Z exchange resulting in different signs of the $\gamma - Z$ interference term. The difference in CC scattering results from dependence on the quark type (u or d -type) and also the chirality dependence. All data sets agree well with the Standard Model (SM) predictions. Since it is evident that the exploration of the high Q^2 region is still statistics limited, the high luminosity phase at HERA II will allow to test this region with much higher precision.

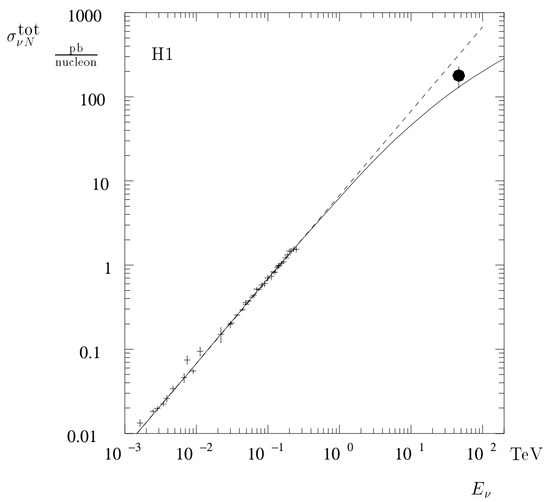

Figure 1. CC crosss sections as function of fixed target lepton energy. Early 1993 HERA data and neutrino data are shown.

1.2. *Combined Electroweak-QCD Analysis*

Using the deep inelastic e^+p and e^-p charged and neutral current scattering cross sections derived from HERA I data, H1 performed a combined electroweak and QCD analysis [4] in order to determine electroweak parameters accounting for their correlation with parton distributions. The basis for this combined EW-QCD analysis is the H1 QCD analysis, the so-called H1PDF2000 [2]. In that analysis the cross sections were fitted describing the parton distributions by 10 free parameters while fixing the electroweak parameters to their SM values. In the new combined EW-QCD anlaysis in addition the electroweak parameters are fitted.

The additional free parameters depend on the choice of the electroweak

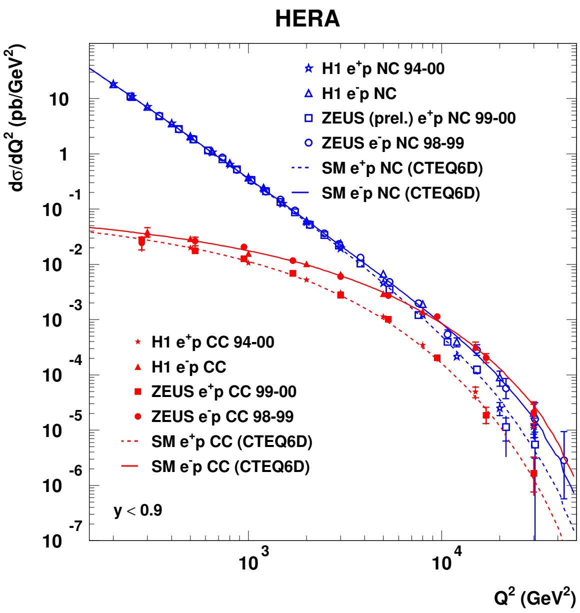

Figure 2. Differential cross section for NC and CC e^+-p and e^--p scattering.

renormalization scheme. The On-Mass-Shell scheme (OMS) uses the weak boson masses as fundamental parameters. In the Modified-On-Mass-Shell scheme (MOMS) the Fermi constant G_F is taken as fundamental parameter instead of M_W.

In the MOMS scheme the CC cross section reads

$$\frac{d^2\sigma^{CC}(e^\pm p)}{dxdQ^2} = \frac{G_F^2}{2\pi x}\left[\frac{M_{prop}^2}{M_{prop}^2 + Q^2}\right]^2 \phi_{CC}^{\pm}(x,Q^2) \tag{1}$$

with $\phi_{CC}^{\pm}(x,Q^2)$ describing the structure function dependences. Here G_F determines the normalization and the W mass entering the formula is the propagator mass M_{prop}. In the first fit performed in the MOMS scheme the parameters G_F and M_{prop} are considered as independent. The result on G_F and M_{prop} in this 12 parameter EW-QCD fit is shown in Figure 3(upper). When in a second fit the well measured Fermi constant is fixed to its PDG value the propagator mass is found to be

$$M_{\rm prop} = 82.87 \pm 1.82_{\rm exp}\ {}^{+0.30}_{-0.16}\big|_{\rm model}\ {\rm GeV}\,. \tag{2}$$

Here the first error is experimental and the second corresponds to uncertainties due to input parameters and model assumptions. The propagator mass is within errors consistent with the W mass as measured at LEP and the Tevatron.

Within the OMS scheme the Fermi constant G_F is expressed by

$$G_F = \frac{\pi\alpha}{\sqrt{2}M_W^2\left(1-\frac{M_W^2}{M_Z^2}\right)}\frac{1}{1-\Delta r}\,, \tag{3}$$

where $\alpha \equiv \alpha(Q^2 = 0)$ is the fine structure constant and the term Δr contains the electroweak radiative corrections, sensitive to the Higgs and top masses. In the OMS scheme the W mass is determined from the normalization of the CC cross section, in this case being however sensitive to the parameters (M_H, M_t) in the electroweak radiative corrections. Fixing $M_H = 120\,\text{GeV}$ gives for M_t and M_W the result shown in Figure 3(lower). Fixing M_t to its world average value of 178 GeV leads to

$$M_W = 80.786 \pm 0.205_{\text{exp}}\, {}^{+0.048}_{-0.029}\big|_{\text{model}} \pm 0.025_{\delta m_t} - 0.084_{\delta M_H} \pm 0.033_{\delta(\Delta r)}\,\text{GeV}\,. \tag{4}$$

Here, in addition to the experimental and model uncertainties, three other error sources are considered, the uncertainty on the top quark mass $\delta m_t = 4.3\,\text{GeV}$, a variation of the Higgs mass from 120 GeV to 300 GeV and the uncertainty of higher-order terms.

At HERA the NC interactions at high Q^2 receive contributions from γ and Z exchange. Thus the NC data can be used to extract the weak couplings of up- and down-type quarks to the Z boson. At high Q^2 and high x, where the NC $e^{\pm}p$ cross sections are sensitive to these couplings, the up- and down-type quark distributions are dominated by the light u and d quarks. Therefore, this measurement can be considered to determine the light quark couplings. The CC cross section data help disentangle the up and down quark distributions. In this analysis the vector and axial-vector couplings v_u-a_u-v_d-a_d of u and d quarks are treated as free parameters. The results of the EW-QCD fit are shown in Fig. 4. The measured couplings are in good agreement with the SM expectations. The results are compared in Figure 4 with similar results obtained from the combined LEP data [5]. The HERA results resolve the sign ambiguity inherent in the LEP results.

2. Results from HERA II

The HERA accelerator and the experiments have undergone major modifications in the years 2000-2002 in order to achieve significantly higher

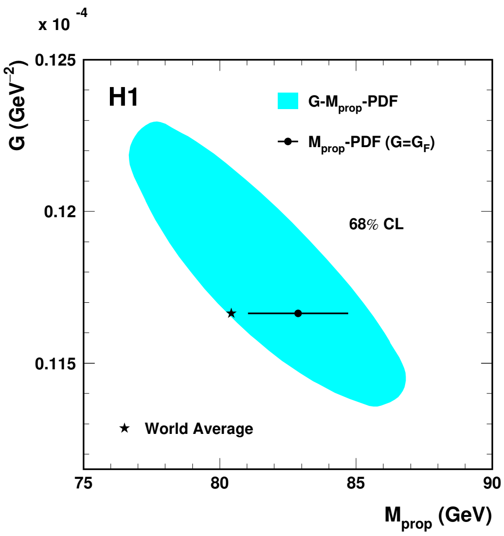

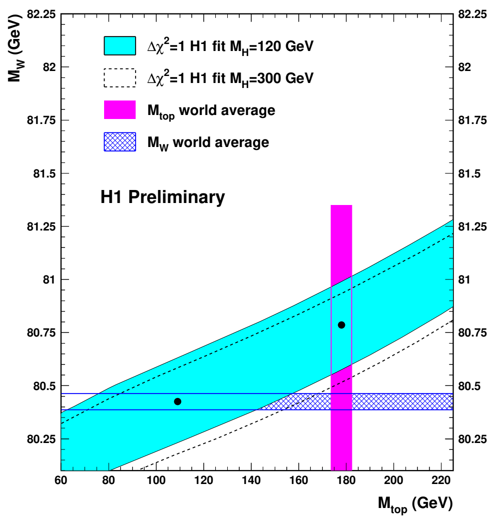

Figure 3. Upper figure : Result of the fit to G_F and M_{prop} (MOMS scheme). Lower figure : Result of the fit to M_t and M_W (OMS scheme).

luminosities. It is planned to accumulate around 700 pb^{-1} per experiment in the HERA II phase (up to 2007). This will significantly reduce the statistical errors in the high Q^2 region which is important for electroweak

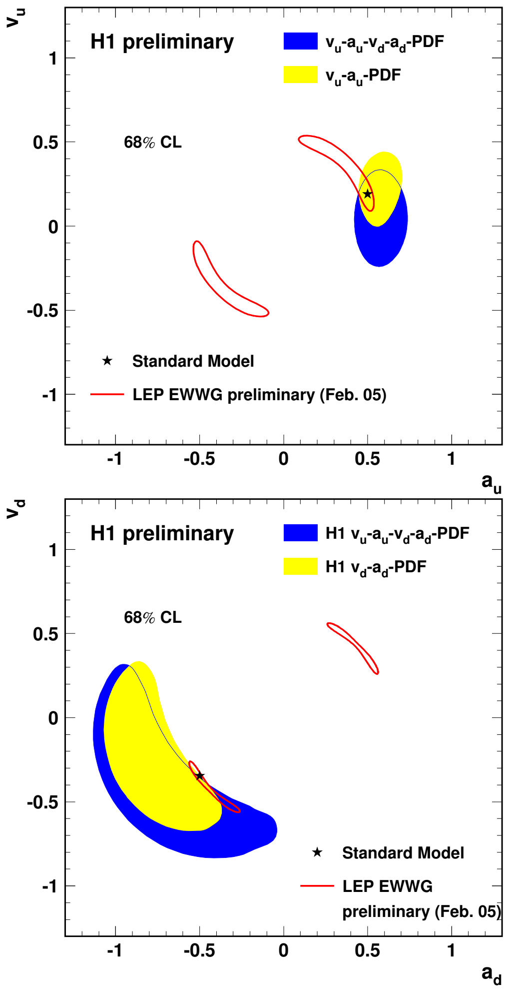

Figure 4. Results on the weak NC Z couplings to u (upper fig.) and d (lower fig.) quarks. The results from LEP are also shown.

physics studies. Another important aspect for electroweak physics is the availibility of longitudinally polarised leptons in the HERA II phase.

2.1. *Polarised CC cross sections*

The first physics analysis making use of the lepton polarisation is the measurement of the CC cross sections as a funtion of the degree of lepton polarisation. The double differential CC cross section for collisions of polarised leptons with unpolarised protons can be written as

$$\frac{d^2\sigma_{CC}^{e^\pm p}}{dxdQ^2} = [1 \pm P_e]\frac{G_F^2}{2\pi x}[\frac{M_W^2}{Q^2 + M_W^2}]^2\Phi_{CC}^{\pm}, \tag{5}$$

Here, P_e is the degree of longitudinal polarisation defined as $P_e = (N_R - N_L)/(N_R + N_L)$ with $N_R(N_L)$ being the number of right (left) handed polarised leptons in the beam. The cross section has a linear dependence on the lepton polarisation and vanishes for lefthanded positrons and for righthanded electrons due to the V-A structure of the CC interaction.

Both collaborations used the data accumulated in 2003-2005 with polarised e^+ and e^- and combined these with the unpolarised data taken in the HERA I phase. The luminosities analysed up to now with polarised beams are relatively small (typically 10-30 pb^{-1} per charge and polarisation state) and the degree of polarisation is only 30-40 %. Nevertheless both collaborations presented in their preliminary analyses for the 2005 summer conferences [6,7] clear evidence for the V-A structure of high Q^2 CC interactions.

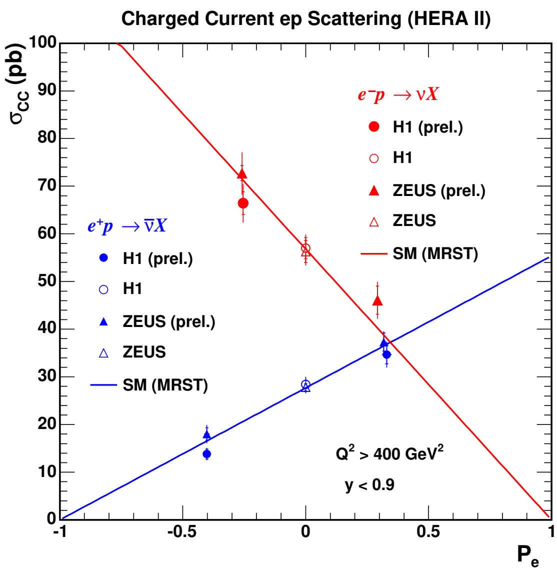

Figure 5. Total CC cross section for e^+p and e^-p scattering as function of the degree of longitudinal lepton polarisation. P

Fig 5 shows the CC cross sections for e^+p and e^-p scattering in the region $Q^2 > 400\,\mathrm{GeV}^2$ and $y < 0.9$ as function of the degree of longitudinal polarisation P. The data clearly exhibit the linear dependence with P and are compatible with vanishing cross sections for left(right)-handed positrons(electrons). Fitting a linear dependence to the e^+p data results in an extrapolated cross section of $\sigma_{CC}^{e^+}(P=-1) = 0.2 \pm 1.8(stat) \pm 1.6(syst)$ pb, consistent with the SM prediction of zero.

The ZEUS collaboration measured also polarisation dependences of differential CC crosss sections [7]. Fig 6 shows these as funtion of the kinematic variables x, y and Q^2 for the case of e^-p scattering. As expected, all cross sections scale linearly with polarisation.

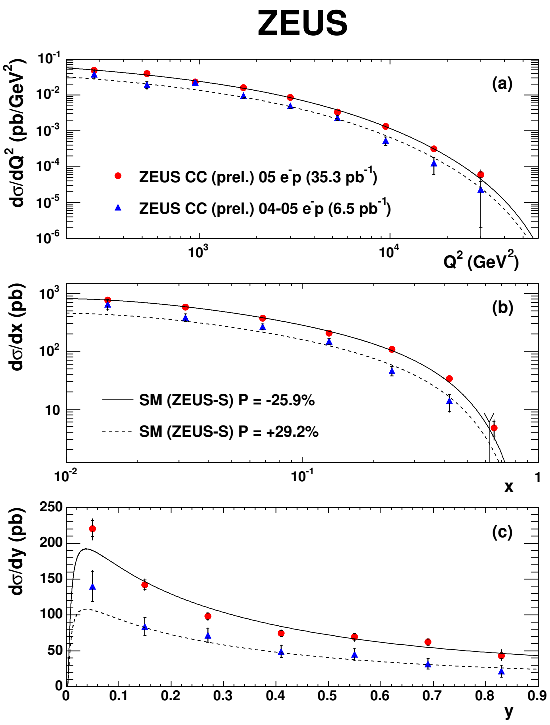

Figure 6. Differential CC e^--p cross sections for two polarisation states

2.2. *Polarised NC cross sections*

The dependence of NC cross sections on the polarisation is more involved due to the contribution of γ and Z exchange in the amplitudes and the different chirality couplings. The bulk of the cross sections is dominated by γ exchange and thus independent of P and equal for e^+p and e^-p scattering. Only at highest Q^2 sensitivity to polarisation shows up due to the onset of the $\gamma - Z$ interference. Figure 7 shows the ZEUS results [7] for the dependence of the NC cross section on Q^2 for two polarisation states. The bottom part of the figure shows the cross section ratio for the two polarisations. Although the polarisation dependence is not observed conclusively, it is well compatible with the expected SM behaviour.

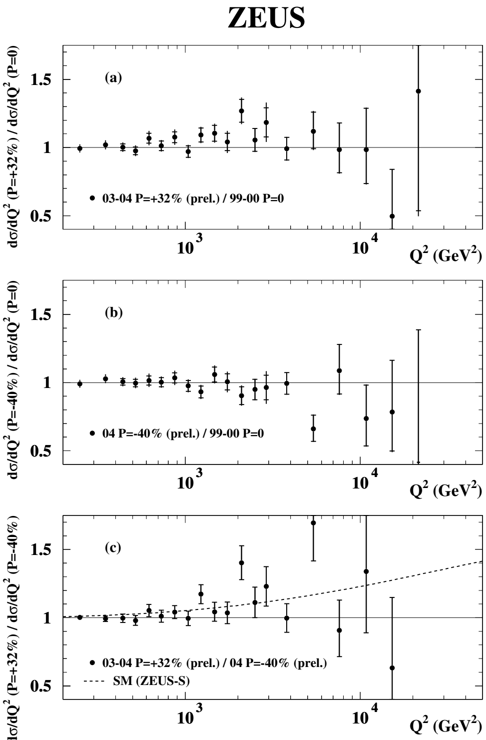

Figure 7. Differential NC e^+-p cross sections for two polarisation states normalized to the unpolarised one a),b). In c) the cross section ratio for the two polarisation states is shown.

Summary

Many aspects of electroweak physics have been studied at HERA. In the HERA-I phase with unpolarised leptons luminosities $\sim 100\,\mathrm{pb}^{-1}$ per experiment have been analysed. The measured NC and CC cross section provide clear evidence for electroweak unification as predicted in the SM. In global fits to the structure functions electroweak parameters (M_{prop}, M_W and the vector and axialvector couplings of the Z to up and down quarks) are determined. All results are in agreement with the SM predictions.

The newly available longitudinal lepton polarisation enhances the potential of electroweak measurements at HERA significantly. Already the very first analyses based on relatively low luminosity samples give encouraging results. The highlight here is the demonstration of the V-A structure of the charged current interaction at the very high spacelike momentum transfers never exploited before in deep inelastic scattering.

Since all results at high Q^2 are presently statistics limited the high luminosity expected to be accumulated until the end of HERA operation promises exciting physics results to come.

Acknowledgments

I like to thank the organisers of this workshop for the very stimulating atmosphere at Ringberg.

References

1. T. Ahmed et al. [H1 Collaboration], *Phys. Lett.* **B324**, 241 (1994).
2. C. Adloff et al. [H1 Collaboration] *Eur.Phys.J* **C30**, 1 (2003).
3. S. Chekanov et al. [ZEUS Collaboration] *Eur.Phys.J* **C32**, 1 (2003).
   S. Chekanov et al. [ZEUS Collaboration] *Phys.Rev.* **D70**, 052001 (2004).
4. A. Aktas et al. [H1 Collaboration] Accepted by *Phys. Lett.* , hep-ex/0507080 (2005).
5. LEP and SLD Electroweak Working Groups, http://lepewwg.web.cern.ch/LEPEWWG/plots/winter2005/
6. H1 Collaboration, contributed paper LP2005 (2005), Uppsala , abstract 388
   H1 Collaboration, contributed paper ICHEP04(2004), Beijing, abstract 756,758
7. ZEUS Collaboration , contributed papers LP2005 (2005), Uppsala , abstracts 254 and 255